Discovery of the Novel Antithrombotic Agent 5-Chloro-*N*-({(5*S*)-2-oxo-3-[4-(3-oxomorpholin-4-yl)phenyl]-1,3-oxazolidin-5-yl}methyl)thiophene-2-carboxamide (BAY 59-7939): An Oral, Direct Factor Xa Inhibitor

Susanne Roehrig,* Alexander Straub,‡ Jens Pohlmann,# Thomas Lampe, Josef Pernerstorfer, Karl-Heinz Schlemmer, Peter Reinemer,§ and Elisabeth Perzborn

Bayer HealthCare AG, D-42096 Wuppertal, Germany

Received February 2, 2005

Despite recent progress in antithrombotic therapy, there is still an unmet medical need for safe and orally available anticoagulants. The coagulation enzyme Factor Xa (FXa) is a particularly promising target, and recent efforts in this field have focused on the identification of small-molecule inhibitors with good oral bioavailability. We identified oxazolidinone derivatives as a new class of potent FXa inhibitors. Lead optimization led to the discovery of BAY 59-7939 (**5**), a highly potent and selective, direct FXa inhibitor with excellent in vivo antithrombotic activity. The X-ray crystal structure of **5** in complex with human FXa clarified the binding mode and the stringent requirements for high affinity. The interaction of the neutral ligand chlorothiophene in the S1 subsite allows for the combination of good oral bioavailability and high potency for nonbasic **5**. Compound **5** is currently under clinical development for the prevention and treatment of thromboembolic diseases.

Introduction

The activated serine protease Factor Xa (FXa) plays a central role in the blood coagulation cascade, as it is activated by both the intrinsic and the extrinsic pathways. FXa catalyzes the conversion of prothrombin to thrombin through the prothrombinase complex, which consists of FXa, FVa, prothrombin, and Ca^{2+} on a phospholipid surface.[1] Thrombin has several thrombotic functions, including the conversion of fibrinogen to fibrin, the activation of platelets, and the feedback activation of other coagulation factors, resulting in the amplification of its own formation. Inhibition of FXa produces antithrombotic effects by decreasing this amplified generation of thrombin, thus diminishing thrombin-mediated activation of both coagulation and platelets, without affecting existing thrombin levels. This remaining thrombin should be sufficient to ensure primary hemostasis, resulting in a favorable safety margin.[2] Therefore, FXa is a particularly promising target for anticoagulant therapy and has attracted great interest in recent years.[3] A significant advantage over current antithrombotic therapies[4] should be provided by a small-molecule, direct FXa inhibitor that can be administered orally without the need for routine coagulation monitoring.

In this paper, we show that oxazolidinone derivatives represent a new class of highly potent FXa inhibitors. We discovered compound **5**, a potent and selective, direct FXa inhibitor with excellent in vivo activity and good oral bioavailability, which is currently under clinical development for the prevention and treatment of thromboembolic diseases. We report on the structure−activity relationship (SAR) around **5**, its synthesis, and binding mode in cocrystallization with human FXa.

Structure−Activity Relationship and Pharmacological Activity. Our program started with the optimization of the lead compound **1** (IC_{50} 120 nM), derived from high throughput screening (HTS), yielding isoindolinones (e.g. **2**, IC_{50} 8 nM) as potent FXa inhibitors (Figure 1).[5] Within this series, we could not achieve the target pharmacokinetic profile, as compounds with sufficient potency generally showed low bioavailabilities due to low absorption. But we learned that the 5-chlorothiophene-2-carboxamide moiety was essential for potent FXa inhibition. When reevaluating the HTS hits by similarity considerations, we identified the oxazolidinone **3** as a very weak FXa inhibitor (IC_{50} 20 μM). Applying our experience of the isoindolinone class, exchange of the thiophene moiety in **3** with 5-chlorothiophene provided the lead compound **4** with more than 200-fold improved potency (IC_{50} 90 nM). A clear preference for (*S*)-configuration at the oxazolidinone core was observed, indicating a specific interaction with FXa. The lead compound **4** offered an excellent starting point for optimization to an orally available FXa inhibitor: this lead did not comprise a highly basic group such as amidine or any other positively charged group; these groups were, for a long time, thought to be essential for interacting in the S1 pocket, but they usually contribute to only poor oral absorption.[6] Furthermore, the oxazolidinone class is generally known for its favorable pharmacokinetic profile.[7] Based on this promising lead, a medicinal chemistry program was initiated to evaluate the SAR and to further improve potency and the pharmacokinetic profile.

We began our investigation with the optimization of the thiomorpholine group (Table 1). Some improvement in FXa inhibition was obtained with the morpholine

* Corresponding author: Phone: +49 202 36 4889. Fax: +49 202 36 4624. E-mail: susanne.roehrig@bayerhealthcare.com.
‡ Current address: Bayer CropScience AG, D-40789 Monheim, Germany.
# Current address: Basilea Pharmaceutica Ltd, CH-4005 Basel, Switzerland.
§ Proteros Biostructures GmbH, D-82152 Martinsried, Germany.

10.1021/jm050101d CCC: $30.25
Published on Web 08/18/2005

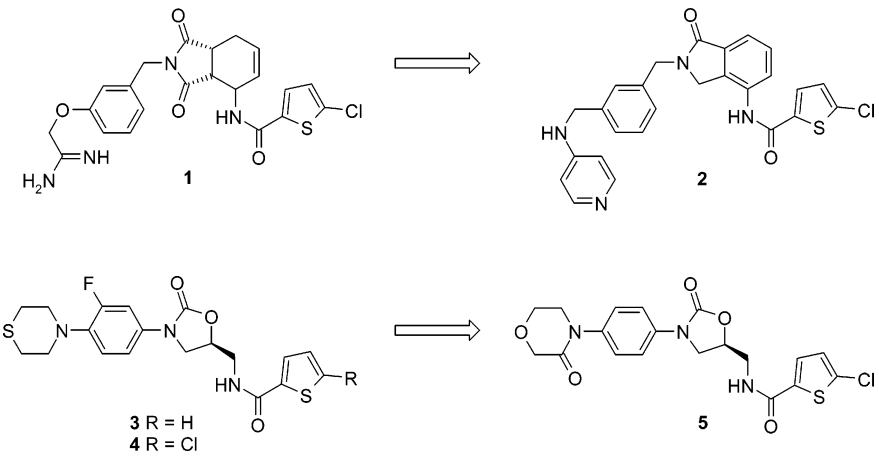

Figure 1. Optimization to oxazolidinone FXa inhibitors.

Table 1. In Vitro Anti-FXa Potency

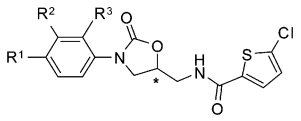

compd	R^1	R^2, R^3	*ent*	IC_{50} [nM]
4		F, H	(*S*)	90
6		F, H	(*S*)	32
7		H, H	(*S*)	43
8		F, H	(*S*)	40
9		H, H	(*S*)	74
10		F, H	(*S*)	140
11		H, H	(*S*)	4.0
5		H, H	(*S*)	0.7
12		F, H	(*S*)	1.4
13		CF_3, H	(*S*)	1.0
14		NH_2, H	(*S*)	2.5
15		H, CH_3	(*S*)	1260
16		H, H	(*R*)	2300

derivative **6** (IC_{50} 32 nM), the nonfluorinated compound **7** (IC_{50} 43 nM), and the pyrrolidine derivative **8** (IC_{50} 40 nM). In contrast, decreased inhibition was observed with the dimethylamino derivative **9** (IC_{50} 74 nM) and the piperazine derivative **10** (IC_{50} 140 nM). Compared with **8**, a significant improvement in potency was obtained with the pyrrolidinone derivative **11** (IC_{50} 4.0 nM). The combination of these results led to the design of the morpholinone derivative **5**, achieving a strong gain in anti-FXa potency (IC_{50} 0.7 nM; K_i 0.4 nM). Within the morpholinone series, substitution at the 3-aryl-position was well tolerated, resulting in compounds with similar potency, such as the 3-fluoro derivative **12** (IC_{50} 1.4 nM), the 3-trifluoromethyl derivative **13** (IC_{50} 1.0 nM), and the 3-amino derivative **14** (IC_{50} 2.5 nM). Substitution at the 2-aryl-position was unfavorable; for example, the 2-methyl derivative **15** (IC_{50} 1.26 μM) showed 30-fold decreased inhibition compared with unsubstituted **7**. The correct configuration at the oxazolidinone ring was essential [IC_{50} value of 0.7 nM for (*S*)-enantiomer[8] **5** vs 2.3 μM for (*R*)-enantiomer **16**].

The lipophilic chlorothiophene moiety was responsible for a decrease in fraction unbound (f_u) and aqueous solubility [f_u (**5** in human plasma): 5.1%;[9] aqueous solubility of crystalline **5**: 8 mg L^{-1}]. Therefore, we tried to identify less lipophilic replacements by broad variation, but we were not successful: we observed a very steep SAR around the chlorothiophene moiety (Table 2). The only subnanomolar inhibitor obtained within this series besides **5** was the 5-bromothiophene derivative **17** (IC_{50} 0.4 nM). The 5-methylthiophene derivative **18** (IC_{50} 4.2 nM) showed decreased potency. The exchange of 5-bromothiophene with 5-bromofuran resulted in a 65-fold weaker inhibition (**19**, IC_{50} 26 nM). The closely related 4-chlorophenyl derivative **20** (IC_{50} 20 nM) was 30-fold less potent than **5**, and moving the chloro substituent to the 3- or 2-position of the aryl ring caused further significant loss in potency (**21**, IC_{50} 1.17 μM; **22**, 2 μM). More polar variations proved to be less favorable; for example, derivative **23** (IC_{50} 8.5 nM) with an additional 4-amino-group showed a decreased inhibition of 12-fold compared with **5**, and the 2-chloro-1,3-thiazole **24** (IC_{50} 290 nM) was more than 400-fold less potent. Within the chloropyridine derivatives, **25** (IC_{50} 29 nM) showed a 40-fold weaker potency compared with **5**, and **26** (IC_{50} 94 nM) was even less potent.

With the 5-chlorothiophene residue identified, the amide linker proved to be optimal. Substitution of the

Table 2. In Vitro Anti-FXa Potency

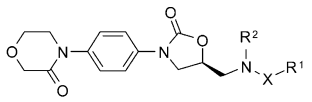

compd	R^1	X	R^2	IC_{50} [nM]
5	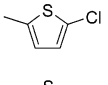	CO	H	0.7
17	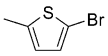	CO	H	0.4
18	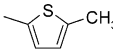	CO	H	4.2
19	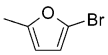	CO	H	26
20	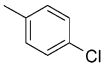	CO	H	20
21	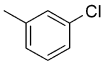	CO	H	1170
22	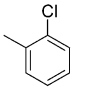	CO	H	2000
23	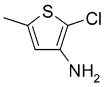	CO	H	8.5
24	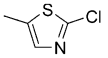	CO	H	290
25	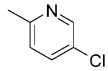	CO	H	29
26	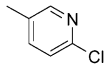	CO	H	94
27	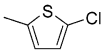	CO	CH_3	197
28	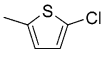	SO_2	H	1200

amide was less favorable, as reflected by the 280-fold decrease in potency when it is methylated (**27**, IC_{50} 197 nM). The corresponding sulfonamide **28** was even less potent (IC_{50} 1.2 μM).

In summary, the combination of the morpholinone and the 5-chlorothiophene-2-carboxamide moiety within the oxazolidinone FXa inhibitors resulted in subnanomolar in vitro potency.

The prolongation of the prothrombin time (PT) was measured for selected compounds to determine their in vitro anticoagulant activity (defined as the inhibitor concentration required to double the time to fibrin formation). In rat plasma, doubling of the PT was obtained at concentrations of 2.8 μM for the pyrrolidinone derivative **11** and of 0.30−0.49 μM for morpholinone derivative **5** and its analogues. In human plasma, PT was doubled at concentrations of 0.40 μM for derivative **11** and of 0.17−0.30 μM for the morpholinone derivatives (Table 3).[10]

The in vivo antithrombotic effect of selected compounds was determined in the arteriovenous (AV) shunt model in anesthetized rats (Table 4).[10] The pyrrolidinone derivative **11** reduced thrombus weight in a dose-dependent manner after intravenous (iv) administration (ED_{50} 7 mg kg^{-1}). Significantly higher in vivo activity was obtained for the morpholinone series than for **11**, which correlated well with the lower concentration required to double the PT in rats. After iv administration, the 3-trifluoromethyl derivative **13** had an ED_{50} value of 3 mg kg^{-1}, whereas both **5** and its 3-fluoroaryl derivative **12** had a lower ED_{50} value of 1 mg kg^{-1}. After oral administration, **12** had an ED_{50} value of 10 mg kg^{-1}, whereas **5** reduced thrombus weight at a lower dose (ED_{50} 5 mg kg^{-1}).

Table 3. In Vitro Prothrombin Time (PT) Assay

compd	$PT2^{human}$ [μM]	$PT2^{rat}$ [μM]
11	0.40	2.8
5	0.23	0.30
12	0.17	0.32
13	0.26	0.32
14	0.30	0.49

PT2 value is defined as the inhibitor concentration required to double the time to fibrin formation.

Table 4. In Vivo Antithrombotic Effect in the Arteriovenous (AV) Shunt Model in Anesthetized Rats

compd	ED_{50}^{iv} [mg kg^{-1}]	ED_{50}^{po} [mg kg^{-1}]
11	7	>30
5	1	5
12	1	10
13	3	n.d.

Table 5. Pharmacokinetic Profile in Male Wistar Rats

compd	CL [L h^{-1} kg^{-1}]	V_{ss} [L kg^{-1}]	$t_{1/2}$ [h]	bioavailability [%]	f_u [%]
11	0.17[a]	0.21	1.1	65[b]	0.2
5	0.40[c]	0.30[c]	0.9[c]	60[d]	1.3
12	1.09[e]	0.32	0.3	n.d.	n.d.

[a] 1 mg kg^{-1} iv [in EtOH/PEG400 (1:9), volume: 1 mL kg^{-1}]. [b] 3 mg kg^{-1} po [in SolutolHS15/EtOH/water (4:1:5), volume: 5 mL kg^{-1}]. [c] Mean values derived by administration of 1 and 3 mg kg^{-1} iv [in PEG400/water (6:4), volume: 5 mL kg^{-1}]. [d] Mean value calculated by dividing the AUC_{norm} after 1, 3, and 10 mg kg^{-1} po [in PEG400/water (6:4), volume: 5 mL kg^{-1}] with the mean AUC_{norm} after iv administration of 1 and 3 mg kg^{-1}. [e] 0.3 mg kg^{-1} iv [in plasma/DMSO (99:1), volume: 2 mL kg^{-1}].

Table 6. Pharmacokinetic Profile in Female Beagle Dogs

compd	CL [L h^{-1} kg^{-1}]	V_{ss} [L kg^{-1}]	$t_{1/2}$ [h]	bioavailability [%]	f_u [%]
5	0.30[a]	0.40[a]	0.9[a]	60−86[b]	10.4

[a] Mean values derived from administration of 0.3 and 1 mg kg^{-1} iv [0.25 h infusion in PEG400/EtOH/water (6:2:2), volume: 0.5 mL kg^{-1}]; [b] Bioavailability range is calculated by dividing the AUC_{norm} after 0.3, 1, and 3 mg kg^{-1} p.o. [in vehicle [a]), volume: 1 mL kg^{-1}] with the AUC_{norm} after iv administration of either 0.3 or 1.0 mg kg^{-1}.

The pharmacokinetic profile in rats was determined for selected compounds (Table 5). The best overall pharmacokinetic profile in rats was achieved with the two compounds **11** and **5**[9]: low clearance of 0.17 L h^{-1} kg^{-1} and 0.40 L h^{-1} kg^{-1}, half-lives of 1.1 and 0.9 h, and good oral bioavailabilities of 65% and 60% were observed, respectively. Higher clearance and shorter half-life were observed for the 3-fluoroaryl analogue of **5**, compound **12**. In dogs, compound **5** showed low plasma clearance of 0.30 L h^{-1} kg^{-1}, half-life of 0.9 h, and moderate to high oral bioavailability of 60−86% (Table 6).[9]

Scheme 1. General Synthetic Pathways for Oxazolidinone Derivatives[a]

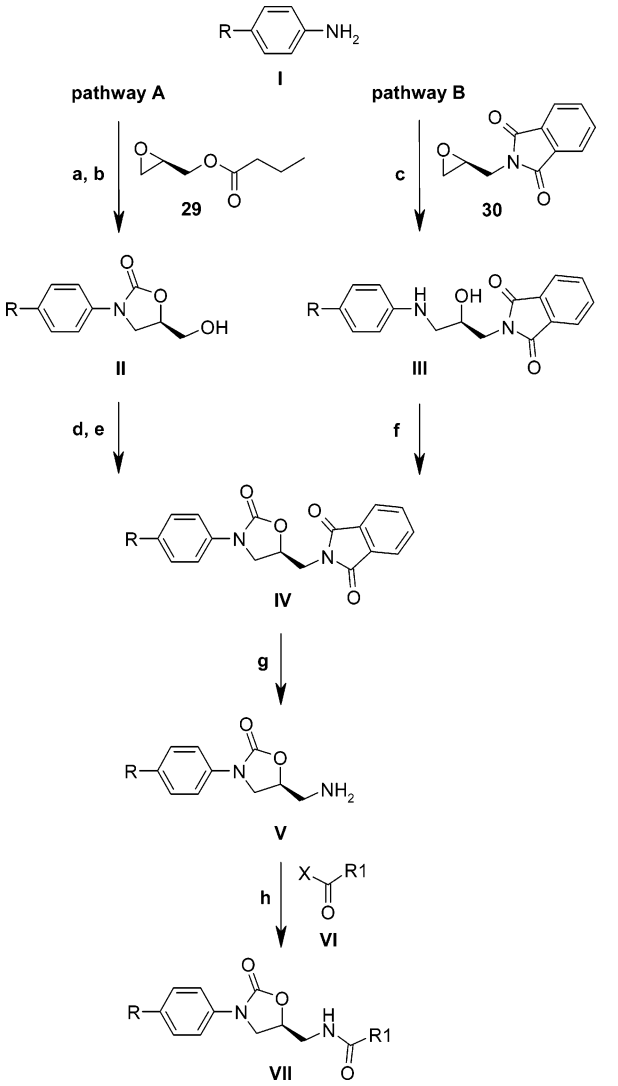

[a] Reagents and conditions: (a) CbzCl, THF, −20 °C; (b) *n*-BuLi, THF, −78 °C to room temperature; (c) EtOH/H_2O (9:1), reflux; (d) MsCl, NEt_3, CH_2Cl_2, 0 °C to room temperature; (e) potassium phthalimide, CH_3CN; (f) *N,N′*-carbonyldiimidazole (CDI), DMAP, THF, reflux; (g) $MeNH_2$, MeOH, reflux or $N_2H_4 \cdot H_2O$, MeOH, reflux; (h) X = Cl: pyridine, THF, 0 °C to room temperature; X = OH: HOBt, EDCI, DIEA, DMF, room temperature.

Compound **5** did not affect related serine proteases (such as thrombin, trypsin, plasmin, FVIIa, FIXa, FXIa, urokinase, and activated protein C) at concentrations up to 20 μM, demonstrating more than 10 000-fold higher selectivity for FXa than for these other serine proteases. Thus, with its excellent in vitro and in vivo efficacy and good pharmacokinetic profile, compound **5** was identified as the leading candidate and was selected for clinical development.

Chemistry. The oxazolidinones **VII** were synthesized as shown in Scheme 1. Two synthetic pathways are described, and pathway B is used where aniline substituents (R) are not compatible with *n*-butyllithium. The desired stereochemistry was introduced via commercially available (*R*)-(−)-glycidol butyrate (**29**) or phthalimide-protected epoxide **30**[11] derived from (*S*)-(−)-glycidol. In pathway A, aniline **I** was first Cbz-protected and then converted to the oxazolidinone **II** with (*R*)-(−)-glycidol butyrate in the presence of *n*-butyllithium.[12] The resultant alcohol **II** was then transformed into the corresponding amine **V** via introduction of phthalimide and subsequent deprotection. Acylation of **V** provided the desired oxazolidinone **VII**. In pathway B, the phthalimide-protected oxazolidinone **IV** was obtained by opening of epoxide **30** with aniline **I** and subsequent ring closure with *N,N′*-carbonyldiimidazole (CDI).

Compound **5** was synthesized following pathway B as shown in more detail in Scheme 2. Opening of epoxide **30** with 4-(4-aminophenyl)morpholin-3-one (**31**)[13] provided the amino alcohol **32**, which was subsequently converted to the oxazolidinone **33** via ring closure with CDI. After deprotection of the phthalimide with methylamine, amine **34** was acylated with 5-chlorothiophene-2-carbonyl chloride (**35**)[14]. This synthesis afforded **5** with retaining the enantiomeric excess of 99%, introduced by starting material **30**.

X-ray Crystallography. The X-ray crystal structure of **5** in complex with human FXa,[15] obtained at a resolution of 2.08 Å, clarified the binding mode and the stringent requirements for high affinity observed within the oxazolidinone series.

Compound **5** forms two hydrogen bonds to Gly219: a strong hydrogen bond (2.0 Å) from the carbonyl oxygen of the oxazolidinone core and a weaker one (3.3 Å) from the NH group of the chlorothiophenecarboxamide (Figure 2). Supported by these two hydrogen bonds, the (*S*)-oxazolidinone core provides the L-shape needed for FXa binding. It serves as a central template for directing its substituents into the S1 and S4 subsites, a binding mode typical of synthetic direct FXa inhibitors. As shown by the X-ray structure, the oxazolidinone core and the aryl ring are coplanar. Substitution at the 2-aryl-position tends to force the two rings into an unfavorable twisted arrangement. The resulting decrease in affinity was demonstrated experimentally; for example, the methyl-substituted derivative **15** is 30-fold less potent than its unsubstituted analogue **7**.

The S4 pocket in FXa is a narrow hydrophobic channel defined by the aromatic rings of Tyr99, Phe174, and Trp215. The nonpolar aryl ring of **5** extends across the face of Trp215, and the morpholinone moiety is sandwiched between Tyr99 and Phe174. The carbonyl group of the morpholinone does not appear to interact directly with FXa, but rather effects a planarization of the morpholinone ring and brings it into a perpendicular arrangement to the aryl ring. This effect is reflected by the 60-fold higher potency of the morpholinone analogue **5** compared with the morpholine derivative **7**.

The key interaction of **5** with FXa in the S1 pocket involves the chlorothiophene moiety: its chlorine substituent interacts with the aromatic ring of Tyr228 located at the bottom of the S1 pocket. A similar binding mode has been reported for other inhibitors of FXa,[16,17] and for inhibitors of thrombin[18] and trypsin[19]. As a result of this chlorine-Tyr228 interaction in S1, highly basic groups such as amidine or other positively charged groups are not required for high FXa affinity. These groups are designed as arginine-P1 mimics to contribute significantly to potency via a direct electrostatic interaction with Asp189,[20] but they are generally critical for oral bioavailability. Thus, the chlorine-Tyr228 interac-

Scheme 2. Synthesis of **5**[a]

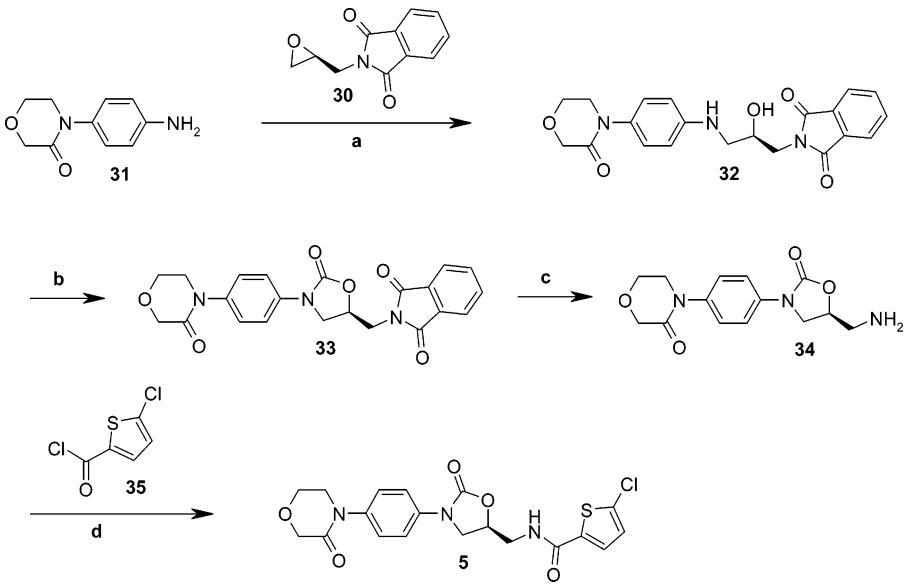

[a] Reagents and conditions: (a) EtOH/H_2O (9:1), reflux, 92%; (b) *N,N′*-carbonyldiimidazole (CDI), DMAP, THF, reflux, 87%; (c) $MeNH_2$, MeOH, reflux; (d) pyridine, THF, 0 °C, 86%.

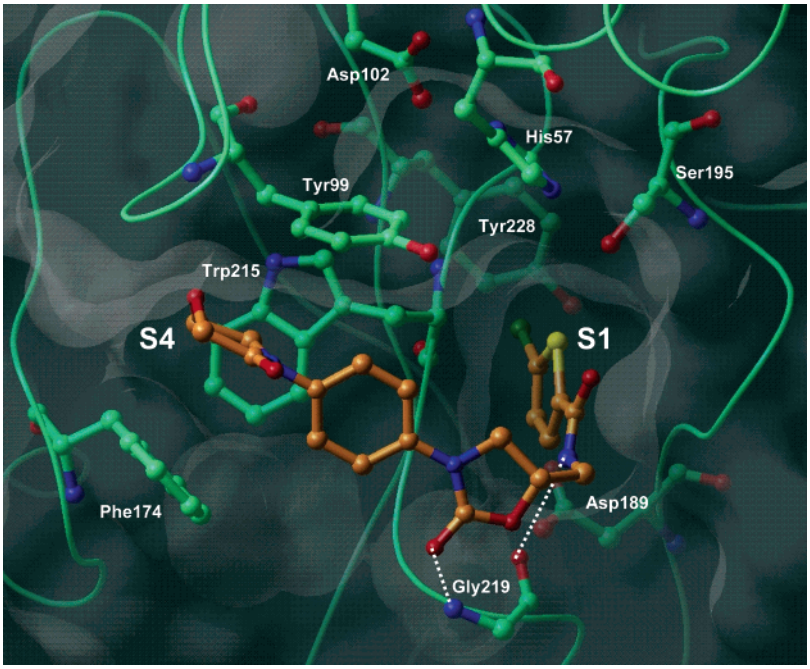

Figure 2. X-ray crystal structure of **5** (orange carbons) in complex with human FXa. Essential amino acids and binding pockets are indicated; the two hydrogen bonds between **5** and Gly219 are shown as doted lines.

tion enabled the combination of high potency and good oral bioavailability for nonbasic **5**.

Conclusion

We showed that the oxazolidinones represent a new class of highly potent FXa inhibitors. Optimization of the lead compound **4** resulted in the identification of the morpholinone derivative **5** with subnanomolar anti-FXa potency. Careful SAR investigation revealed a very steep SAR around its 5-chlorothiophenecarboxamide moiety.

High selectivity of **5** for FXa compared with a range of related serine proteases was observed (>10 000-fold). In an AV-shunt model in rats, the in vivo antithrombotic effect of **5** was demonstrated after oral administration (ED_{50} 5.0 mg kg^{-1}). The pharmacokinetic profile of **5** in rats and dogs showed low clearance and moderate to high oral bioavailability of 60−86%.

The X-ray crystal structure of **5** in human FXa clarified the binding mode and the stringent requirements for high affinity. Supported by two hydrogen bonds to Gly219, the oxazolidinone ring serves as a central core for directing the morpholinone residue into the S4 pocket and the chlorothiophene moiety into the S1 pocket. The key interaction in the S1 pocket involves interaction of the chlorine atom with the aromatic ring of Tyr228. Since this mode of interaction does not require a basic or positively charged group, good oral bioavailability combined with high potency was achieved with nonbasic **5**.

With its excellent in vitro and in vivo efficacy and the good pharmacokinetic profile, **5** was identified as the leading candidate and was selected for clinical development for the prevention and treatment of thromboembolic diseases.

Experimental Section

Pharmacology. In Vitro Studies: FXa and Related Serine Proteases. The enzymatic activity against human FVIIa, FIXa, FXa, FXIa, thrombin, plasmin, trypsin, urokinase, and activated protein C was measured using chromogenic or fluorogenic substrates in 96-well microtiter plates at 25 °C. The enzymes were incubated with the test compound or its solvent (DMSO) for 10 min, and the reactions were initiated by the addition of the appropriate substrate. Color change was monitored continuously at 405 nm by a Spectra Rainbow Thermo Reader (Tecan), and fluorescence was measured at 360/465 nm by a SPECTRAFluor Plus microplate reader (Tecan). Substrates and enzymes were dissolved in aqua bidest or the appropriate assay buffer.

Prothrombin Time (PT) Assay. Commercially available kits were used to measure PT. Clotting times were measured in a coagulometer (Biomatic 4000, Sarstedt), according to the manufacturer's instructions. Increasing concentrations of inhibitor or solvent were added to plasma and incubated for 10 min at 37 °C. Clotting times were measured and compared with those from the appropriate control plasma.

In Vivo Studies: Arteriovenous (AV) Shunt Model. The antithrombotic activity was determined in an AV shunt in anesthetized rats, as described previously[21] with minor modifications: The right common carotid artery and the left jugular vein were cannulated with two 100 mm-long, saline-filled, polyethylene catheters (PE-60, Becton Dickinson). The catheters were connected with a 30 mm-long polyethylene tube (PE-160, Becton Dickinson) containing a rough nylon thread (40 mm × 0.15 mm), folded to create a 20 mm-long double string. The test compound dissolved in poly(ethylene glycol)/water/glycerol (996 g/100 g/60 g) or vehicle was given by intravenous bolus injection into a tail vein 10 min before thrombus induction. Alternatively, the test compound dissolved in solutol/ethanol/water (40%/10%/50% [v/v/v]) or vehicle was administered orally 90 min before thrombus induction. The shunt was opened for 15 min, and the nylon thread covered with the thrombus was then withdrawn and weighed. Blood samples were withdrawn from the carotid artery just after thrombus removal.

In Vitro Plasma-Protein Binding. In vitro plasma-protein binding was evaluated by an equilibrium dialysis method (Scholtan 1962). [^{14}C]-**5** was added to each aliquot of rat, dog, and human plasma to make target concentrations of 0.1, 1.0, 3.0, 10, 30, and 100 mg L^{-1}; in addition, a target concentration of 400 mg L^{-1} was prepared, but only for human plasma. After incubation for 15 min at 37 °C, 0.8 mL of the spiked plasma was dialyzed with an equal volume of phosphate-buffered isotonic solution (PBS, pH 7.4) for 1 h at 37 °C in an equilibrium dialyzer (Dianorm Dialyzer, Dianorm GmbH [Munich, Germany]) equipped with 0.8 mL Teflon half cells separated by a cellulose membrane (Diachema 10.14 cellulose membrane, MWCO 5000 kDa; Dianorm GmbH). The radioactivity of [^{14}C]-**5** in the buffer and the plasma was determined by LSC. The fraction of unbound **5** (f_u [%]) was calculated as follows: $f_u = c_u/c \times 100$, where c_u is the concentration of unbound **5** and c is the total concentration of **5**.

X-ray Crystallography. The X-ray crystal structure of **5** in complex with human FXa was performed by Proteros Biostructures GmbH in Planegg-Martinsried, Germany. Crystals of human FXa in complex with **5** were prepared as described with small modifications.[22] Synchrotron data to 2.08 Å were collected at the Swiss Light Source (SLS) in Villigen at 100 K. Data were integrated, scaled, and merged using XDS. Structure solution was done by molecular replacement using 1EQZ coordinates from PDB as the search model. The model was refined with CNX, using data between 20.0 and 2.08 Å. Diffraction data statistics and structure parameters are shown in Table 7.

Table 7. Diffraction Data Statistics and Structure Parameters

A. Diffraction Data	
wavelength	0.979 Å
space group	$P2_12_12_1$
unit cell parameters	a = 56.04 Å, b = 72.03 Å, c = 78.45 Å $\alpha = \beta = \gamma = 90°$
diffraction limits (highest shell)	20.0−2.08 (2.17−2.08) Å
no. of unique reflections (highest shell)	18555 (1647)
data completeness (highest shell)	94.3% (71.5%)
I/σ_I (highest shell)	12.6 (3.2)
R_{merge}[a]	8.0% (48.2%)
B. Structure Parameters	
no. of non-H atoms in protein	2195
no. of non-H atoms in inhibitor	29
no. of refined water molecules	105
rmsd bond distances from ideal	0.011
rmsd angles from ideal	1.558
crystallographic residual R factor[b]	0.220
crystallographic residual R_{free} factor[b] (test set, 10% of all reflections)	0.259

[a] $R_{merge} = \Sigma_h\Sigma_i|I(h,i) - \langle I(h)\rangle|/\Sigma_h I(h,i)$ where $I(h,i)$ is the intensity value of the i-th measurement of h and $\langle I(h)\rangle$ is the corresponding mean value of h for all i measurements of h; summation is over all measurements [b] $R = \Sigma_{hkl} ||F_o| - |F_c||/\Sigma_{hkl}|F_o|$

Chemistry. General. Unless otherwise noted, all nonaqueous reactions were carried out under an argon atmosphere with commercial-grade reagents and solvents. Melting points (uncorrected) were determined in open capillaries using a Büchi 530 apparatus. NMR spectra were recorded on Bruker Avance spectrometer. Chemical shifts are reported in ppm relative to tetramethylsilane as an internal standard. Mass spectra were obtained on PE SIEX API 150 (ESIpos) or on AMD M40-DF (DCI). High-resolution mass spectra (HR MS) were acquired on a Waters LTC. Analytical HPLC was performed using Hewlett-Packard 1100 instruments under the following conditions: UV detection at 210 nm; column: Reprosil ODS-A 5 μm, 250 mm × 4 mm, temperature: 25 °C, flow: 1.0 mL min^{-1}, eluents: A: water, B: acetonitrile, [method 1a]: isocratic 50%/50%, [method 1b]: isocratic 60%/40%; column: Inertsil Phenyl 5 μm, 250 mm × 3 mm, temperature: 25 °C, flow: 0.6 mL min^{-1}, eluents: A: water, B: acetonitrile, [method 2]: isocratic 60%/40%; column: Kromasil C18, 60 mm × 2 mm, temperature: 30 °C, flow: 0.75 mL min^{-1}, eluents: A: 0.01 M H_3PO_4, B: acetonitrile, [method 3]: gradient: 0−0.5 min 90%A, 0.5−4.5 min 90% → 10%A, 4.5−6.5 min 10%A, 6.5−7.5 min 90%A; column: Kromasil C18, 60 mm × 2 mm, temperature: 30 °C, flow: 0.75 mL min^{-1}, eluents: A: 5 mL 70% $HClO_4$ in 1 L water, B: acetonitrile, [method 4a]: gradient: 0−0.5 min 98%A, 0.5−4.5 min 98% → 10%A, 4.5−6.5 min 10%A, 6.5−6.7 min 10% → 98%A, 6.7−7.5 min 98%A; [method 4b]: gradient: 0−0.5 min 98%A, 0.5−4.5 min 98% → 10%A, 4.5−9.0 min 10%A, 9.0−9.2 min 10% → 98%A, 9.2−10.0 min 98%A. Flash chromatography was performed using silica gel 60 (230−400 mesh). HPLC purifications were performed using RP phase (250 mm × 30 mm GROM-SIL 120, ODS-4HE 10 μm).

5-Chloro-*N*-({(5*S*)-2-oxo-3-[4-(3-oxomorpholin-4-yl)phenyl]-1,3-oxazolidin-5-yl}methyl)thiophene-2-carboxamide (5). (a) 2-((2*R*)-2-Hydroxy-3-{[4-(3-oxomorpholin-4-yl)-phenyl]amino}propyl)-1*H*-isoindole-1,3(2*H*)-dione (32). A suspension of 2-[(2*S*)-oxiran-2-ylmethyl]-1*H*-isoindole-1,3(2*H*)-dione[11] (**30**) (5.7 g, 27.9 mmol) and 4-(4-aminophenyl)morpholin-3-one[13] (**31**) (5.4 g, 27.9 mmol) in ethanol/water (9:1, 140 mL) was refluxed for 14 h. The starting material slowly dissolved, and the product then precipitated from the solution. The precipitate was filtered, washed with diethyl ether, and dried in vacuo. The combined mother liquids were evaporated, the resulting residue was combined with a second portion of **30** (2.8 g, 14.0 mmol), suspended in ethanol/water (9:1, 70 mL) and refluxed for 13 h. The precipitate was filtered, washed with diethyl ether and dried in vacuo. The combined precipitate afforded the title compound **32** (10.1 g, 92% yield) as a

colorless solid. ^{1}H NMR (DMSO-d_6, 200 MHz): 7.92−7.78 (m, 4H), 7.02 (d, J = 8.8 Hz, 2H), 6.61 (d, J = 8.8 Hz, 2H), 5.65 (t, J = 5.9 Hz, 1H), 5.15 (d, J = 5.2 Hz, 1H), 4.13 (s, 2H), 4.08−3.87 (m, 3H), 3.70−3.53 (m, 4H), 3.26−2.92 (m, 2H); MS (ESIpos): *m/z*: 418 ([M + Na]$^+$, 84%), 396 ([M + H]$^+$, 93%); HPLC: rt (method 4a): 3.34 min (100%).

(b) 2-({(5*S*)-2-Oxo-3-[4-(3-oxomorpholin-4-yl)phenyl]-1,3-oxazolidin-5-yl}methyl)-1*H*-isoindole-1,3(2*H*)-dione (33). *N,N*′-Carbonyldiimidazole (2.9 g, 18.1 mmol) and 4-(dimethylamino)pyridine (catalytic amount) were added to a suspension of **32** (3.6 g, 9.1 mmol) in tetrahydrofuran (90 mL). The reaction mixture was stirred for 12 h at 60 °C, a second portion of *N,N*′-carbonyldiimidazole (2.9 g, 18.1 mmol) was added, and the reaction mixture was stirred for additional 12 h at 60 °C. The precipitate was filtered, washed with tetrahydrofuran, and dried in vacuo. The combined mother liquids were evaporated, and the resulting residue was purified by Flash-LC (mixtures of dichloromethane/methanol). The title compound **33** (3.3 g, 87% yield) was obtained as a colorless solid. ^{1}H NMR (DMSO-d_6, 200 MHz): 7.98−7.80 (m, 4H), 7.53 (d, J = 9.1 Hz, 2H), 7.40 (d, J = 9.1 Hz, 2H), 5.04−4.87 (m, 1H), 4.22 (t, J = 9.1 Hz, 1H), 4.19 (s, 2H), 4.04−3.84 (m, 5H), 3.71 (dd, J = 5.4 Hz, 4.6 Hz, 2H); MS (ESI): *m/z*: 422 ([M + H]$^+$, 100%); HPLC: rt (method 4a): 3.71 min (100%).

(c) 4-{4-[(5*S*)-5-(Aminomethyl)-2-oxo-1,3-oxazolidin-3-yl]phenyl}morpholin-3-one (34). Methylamine (40% in water, 10.2 mL, 0.14 mol) was added to a suspension of **33** (4.5 g, 10.6 mmol) in ethanol (102 mL). The reaction mixture was refluxed for 1 h and evaporated in vacuo. The raw material of **34** was used in the next step without further purification. The raw material can be purified by Flash-LC (mixtures of dichloromethane/methanol) to give the title compound **34** as a colorless solid. ^{1}H NMR (DMSO-d_6, 300 MHz): 7.59 (d, J = 9.1 Hz, 2H), 7.40 (d, J = 9.1 Hz, 2H), 4.67−4.57 (m, 1H), 4.19 (s, 2H), 4.08 (t, J = 8.9 Hz, 1H), 3.97 (dd, J = 5.3 Hz, 3.7 Hz, 2H), 3.87 (dd, J = 8.9 Hz, 6.4 Hz, 1H), 3.71 (dd, J = 5.3 Hz, 3.7 Hz, 2H), 2.90−2.76 (m, 2H), 1.75−1.63 (broad s, 2H); MS (ESIpos): *m/z*: 292 ([M + H]$^+$, 100%); HPLC: rt (method 4a): 2.66 min (98%).

(d) 5-Chloro-*N*-({(5*S*)-2-oxo-3-[4-(3-oxomorpholin-4-yl)-phenyl]-1,3-oxazolidin-5-yl}methyl)-thiophene-2-carboxamide (5). 5-Chlorothiophene-2-carbonyl chloride[14] (**35**) (2.3 g, 12.7 mmol) was added dropwise to a solution of the raw material of **34** in pyridine (90 mL) at 0 °C. The reaction mixture was allowed to warm to room temperature and stirred for 1 h before water was added. After addition of dichloromethane and phase separation, the aqueous phase was extracted with dichloromethane. The combined organic phases were dried (sodium sulfate), filtered, and evaporated in vacuo. The residue was purified by Flash-LC (mixtures of dichloromethane/methanol) to give the title compound **5** (3.9 g, 86% yield) as a colorless solid. mp: 230 °C; ^{1}H NMR (DMSO-d_6, 200 MHz): 8.98 (t, J = 5.8 Hz, 1H), 7.70 (d, J = 4.1 Hz, 1H), 7.56 (d, J = 9.0 Hz, 2H), 7.41 (d, J = 9.0 Hz, 2H), 7.20 (d, J = 4.1 Hz, 1H), 4.93−4.75 (m, 1H), 4.27−4.12 (m, 1H), 4.19 (s, 2H), 4.02−3.91 (m, 2H), 3.84 (dd, J = 9.2 Hz, 6.1 Hz, 1H), 3.76−3.66 (m, 2H), 3.66−3.54 (m, 2H); MS (ESIpos): *m/z*: 436 ([M + H]$^+$, 100%); HR MS ([M + H]$^+$ for $C_{19}H_{18}ClN_3O_5S$): calcd 436.0729, found 436.0726; $[\alpha]_D^{21}$ = −38° (c 0.2985, DMSO); enantiomeric excess: 99% (column: Chiral AD 250 mm × 2 mm, temperature: 50 °C, flow: 0.2 mL min^{-1}, eluent: 10% *n*-heptane/90% ethanol/0.2% TFA, UV: 250 nm); degree of purity: HPLC: rt (method 1b): 5.76 min (100%), rt (method 4a): 3.84 min (100%).

5-Chloro-*N*-({(5*S*)-3-[3-fluoro-4-(3-oxomorpholin-4-yl)-phenyl]-2-oxo-1,3-oxazolidin-5-yl}methyl)thiophene-2-carboxamide (12). Compound **12** was synthesized from 4-(4-amino-2-fluorophenyl)morpholin-3-one[13] according to the procedure described for **5**. ^{1}H NMR (DMSO-d_6, 200 MHz): 8.98 (t, J = 5.7 Hz, 1H), 7.69 (d, J = 4.0 Hz, 1H), 7.58 (dd, J = 12.9 Hz, 2.2 Hz, 1H), 7.47 (d, J = 8.7 Hz, 1H), 7.36 (dd, J = 8.8 Hz, 2.2 Hz, 1H), 7.20 (d, J = 4.0 Hz, 1H), 4.95−4.77 (m, 1H), 4.20 (s, 2H), 4.19 (t, J = 9.0 Hz, 1H), 4.02−3.91 (m, 2H), 3.85 (dd, J = 9.1 Hz, 6.2 Hz, 1H), 3.72−3.52 (m, 4H); MS (ESIpos): *m/z*: 454 ([M + H]$^+$, 53%), 907 ([2M + H]$^+$, 100%); HR MS ([M + H]$^+$ for $C_{19}H_{17}ClFN_3O_5S$): calcd 454.0635, found 454.0620; degree of purity: HPLC: rt (method 1b): 7.58 min (95%), rt (method 2): 6.74 min (95%).

5-Chloro-*N*-({(5*S*)-2-oxo-3-[4-(3-oxomorpholin-4-yl)-3-(trifluoromethyl)phenyl]-1,3-oxazolidin-5-yl}methyl)-thiophene-2-carboxamide (13). Compound **13** was synthesized from 4-[4-amino-2-(trifluoromethyl)phenyl]morpholin-3-one[13] according to the procedure described for **5**. ^{1}H NMR (DMSO-d_6, 300 MHz): 8.93 (t, J = 5.7 Hz, 1H), 8.07−8.00 (m, 1H), 7.84−7.74 (m, 1H), 7.68 (d, J = 4.0 Hz, 1H), 7.59 (d, J = 8.7 Hz, 1H), 7.18 (d, J = 4.0 Hz, 1H), 4.94−4.81 (m, 1H), 4.26 (t, J = 9.1 Hz, 1H), 4.19 (s, 2H), 4.09−3.98 (m, 1H), 3.98−3.86 (m, 2H), 3.75−3.65 (m, 1H), 3.62 (t, J = 5.7 Hz, 2H), 3.53−2.42 (m, 1H); MS (ESIpos): *m/z*: 504 ([M + H]$^+$, 100%); HR MS ([M + H]$^+$ for $C_{20}H_{17}ClF_3N_3O_5S$): calcd 504.0603, found 504.0591; degree of purity: HPLC: rt (method 1b): 12.08 min (100%), rt (method 4b): 4.08 min (100%).

***N*-({(5*S*)-3-[3-Amino-4-(3-oxomorpholin-4-yl)phenyl]-2-oxo-1,3-oxazolidin-5-yl}methyl)-5-chlorothiophene-2-carboxamide (14).** Compound **14** was synthesized from 4-(2,4-diamino-phenyl)morpholin-3-one[13] according to the procedure described for **5**. ^{1}H NMR (DMSO-d_6, 300 MHz): 8.93 (t, J = 5.7 Hz, 1H), 7.68 (d, J = 4.1 Hz, 1H), 7.18 (d, J = 4.0 Hz, 1H), 6.98 (d, J = 2.3 Hz, 1H), 6.97 (d, J = 8.5 Hz, 1H), 6.70 (dd, J = 8.5 Hz, 2.3 Hz, 1H), 5.20−5.10 (broad s, 2H), 4.86−4.75 (m, 1H), 4.23−4.12 (m, 2H), 4.10 (t, J = 9.1 Hz, 1H), 4.05−3.91 (m, 2H), 3.76 (dd, J = 9.1 Hz, 6.0 Hz, 1H), 3.58 (t, J = 5.7 Hz, 2H), 3.53−3.88 (m, 2H); MS (ESIpos): *m/z*: 451 ([M + H]$^+$, 100%); HR MS ([M + H]$^+$ for $C_{19}H_{19}ClN_4O_5S$): calcd 451.0838, found 451.0848; degree of purity: HPLC: rt (method 1b): 4.45 min (98%), rt (method 4a): 3.68 min (100%).

5-Chloro-*N*-({(5*S*)-2-oxo-3-[4-(2-oxopyrrolidin-1-yl)phenyl]-1,3-oxazolidin-5-yl}methyl)thiophene-2-carboxamide (11). Benzyl chloroformate (4.3 g, 25.0 mmol) was slowly added to a solution of 1-(4-aminophenyl)pyrrolidin-2-one[23] (4.0 g, 22.7 mmol) and *N,N*-dimethylaniline (3.6 mL, 28.4 mmol) in tetrahydrofuran (107 mL) at −20 °C. The reaction mixture was stirred for 30 min at −20 °C and then allowed to warm to room temperature. After addition of ethyl acetate and phase separation, the organic phase was washed with saturated brine, dried (magnesium sulfate), filtered, and evaporated in vacuo. The residue was crystallized from diethyl ether to give **benzyl [4-(2-oxopyrrolidin-1-yl)phenyl]carbamate** (5.2 g, 74% yield) as off-white crystals. mp: 174 °C.

n-Butyllithium (2.5 M in hexane) was slowly added to a mixture of isoamyl alcohol (1.5 g, 16.7 mmol) and *N*-benzylidenebenzylamine (one drop, indicator) in tetrahydrofuran (200 mL) at −20 °C until the indicator turned red. The reaction mixture was stirred at −10 °C for 10 min and then cooled to −78 °C. A solution of benzyl [4-(2-oxopyrrolidin-1-yl)phenyl]-carbamate (4.7 g, 15.1 mmol) in tetrahydrofuran (50 mL) was slowly added. Additional *n*-butyllithium (2.5 M in hexane) was added dropwise at −20 °C until the indicator turned pink. The reaction mixture was stirred for 10 min at −78 °C, and (*R*)-glycidol butyrate (2.6 g, 18.2 mmol) was added. After stirring for additional 10 min at −78 °C, the reaction mixture was allowed to slowly warm to room temperature. Water was added, and tetrahydrofuran was evaporated in vacuo. The remaining aqueous solution was extracted with ethyl acetate. The combined organic phases were dried (magnesium sulfate), filtered, and evaporated in vacuo. The residue was crystallized from diethyl ether to give **(5*R*)-5-(hydroxymethyl)-3-[4-(2-oxopyrrolidin-1-yl)phenyl]-1,3-oxazolidin-2-one** (3.76 g, 90% yield) as colorless crystals. mp: 148 °C.

Methanesulfonyl chloride (1.8 g, 15.6 mmol) was added to a solution of (5*R*)-5-(hydroxymethyl)-3-[4-(2-oxopyrrolidin-1-yl)phenyl]-1,3-oxazolidin-2-one (3.6 g, 13.0 mmol) and triethylamine (2.9 g, 28.7 mmol) in dichloromethane (160 mL) at 0 °C. The reaction mixture was stirred at 0 °C for 1.5 h and then at room temperature for 3 h. After addition of water and phase separation, the aqueous phase was extracted with dichloromethane. The combined organic phases were dried (magnesium sulfate), filtered, and evaporated *in* vacuo. The

residue was dissolved in acetonitrile (70 mL), and potassium phthalimide (2.6 g, 14.2 mmol) was added. In a sealed tube, the reaction mixture was placed in the microwave apparatus at 180 °C for 45 min. The reaction mixture was filtered, and the filtrate was concentrated in vacuo. The residue (1.9 g) was dissolved in methanol (35 mL), and hydrazine hydrate (0.47 g, 9.37 mmol) was added. The reaction mixture was refluxed for 2 h and cooled to room temperature. After addition of saturated aqueous sodium bicarbonate and phase separation, the aqueous phase was extracted with dichloromethane. The combined organic phases were dried (magnesium sulfate), filtered, and evaporated in vacuo, yielding **(5*S*)-5-(aminomethyl)-3-[4-(2-oxopyrrolidin-1-yl)phenyl]-1,3-oxazolidin-2-one.**

N′-(3-Dimethylaminopropyl)-*N*-ethylcarbodiimide (0.29 g, 1.51 mmol) and diisopropylethylamine (0.40 mL, 2.32 mmol) were added to a solution of **(5*S*)-5-(aminomethyl)-3-[4-(2-oxopyrrolidin-1-yl)phenyl]-1,3-oxazolidin-2-one** (0.32 g, 1.16 mmol), 5-chlorothiophene-2-carboxylic acid (0.19 g, 1.16 mmol) and 1-hydroxy-1*H*-benzotriazol-hydrate (0.23 g, 1.51 mmol) in dimethylformamide (7.6 mL) at room temperature. The reaction mixture was stirred at room temperature overnight and evaporated in vacuo. The residue was dissolved in dimethyl sulfoxide (3 mL) and purified by HPLC (acetonitrile/water/0.5% TFA gradient). From the combined fractions, acetonitrile was removed and the formed precipitate was filtered to give the title compound **11** (0.19 g, 39% yield) as a colorless solid. mp: 229 °C; ^{1}H NMR (DMSO-d_6, 300 MHz): 8.99 (t, J = 5.7 Hz, 1H), 7.69 (d, J = 4.1 Hz, 1H), 7.67 (d, J = 9.3 Hz, 2H), 7.52 (d, J = 9.3 Hz, 2H), 7.20 (d, J = 4.0 Hz, 1H), 4.89−4.78 (m, 1H), 4.17 (t, J = 9.1 Hz, 1H), 3.88−3.78 (m, 3H), 3.60 (t, J = 5.7 Hz, 2H), 2.45 (m, 2H), 2.05 (m, 2H); MS (ESIpos): 442 ([M + Na]$^+$, 21%), 420 ([M + H]$^+$, 72%), 145 (100%); HR MS ([M + H]$^+$ for $C_{19}H_{18}ClN_3O_4S$): calcd 420.0780, found 420.0786; degree of purity: HPLC: rt (method 1a): 4.54 min (98%), rt (method 4b): 3.92 min (100%).

Acknowledgment. The authors thank Ulrich Rester, Peter Nell, and Axel Jensen for their molecular modeling work and helpful discussion, Axel Harrenga for his support regarding the X-ray crystallography, and the scientists of Proteros Biostructures GmbH in Planegg-Martinsried, Germany, for crystallization, data collection, and structure solution of human FXa in complex with derivative **5**.

Supporting Information Available: Experimental description and analytical data for compounds **4**, **6**−**10**, **15**−**28**. This material is available free of charge via the Internet at http://pubs.acs.org.

References

(1) Mann, K. G.; Jenny, R. J.; Krishnaswamy, S. Cofactor proteins in the assembly and expression of blood clotting enzyme complexes. *Annu. Rev. Biochem.* **1988**, *57*, 915−956.

(2) Numerous animal studies have demonstrated antithrombotic efficacy with FXa inhibitors at doses that have little or no effect on template bleeding times, tail-bleeding time, or cuticle-bleeding times, suggesting a relatively wide therapeutic window between antithrombotic efficacy and bleeding tendency, see for review: Leadley, R. J., Jr. Coagulation factor Xa inhibition: biological background and rationale. *Curr. Top. Med. Chem.* **2001**, *1*, 151−159.

(3) Overviews: (a) Quan, M. L.; Smallheer, J. M. The race to an orally active Factor Xa inhibitor: Recent advances. *Curr. Opin. Drug Discov. Dev.* **2004**, *7*, 460−469. (b) Linkins, L.-A.; Weitz, J. I. New Anticoagulant Therapy. *Annu. Rev. Med.* **2005**, *56*, 63−77. (c) Chang, P. New anticoagulants for venous thromboembolic disease. *IDrugs* **2004**, *7*, 50−57.

(4) (a) Hirsh, J.; Dalen, J.; Anderson, D. R.; Poller, L.; Bussey, H.; Ansell, J.; Deykin, D. Oral anticoagulants: mechanism of action, clinical effectiveness, and optimal therapeutic range. *Chest* **2001**, *119*, 8S−21S. (b) Ansell, J.; Hirsh, J.; Dalen, J.; Bussey, H.; Anderson, D.; Poller, L.; Jacobson, A.; Deykin, D.; Matchar, D. Managing oral anticoagulant therapy. *Chest* **2001**, *119*, 22S−38S. (c) Wells, P. S.; Holbrook, A. M.; Crowther, N. R.; Hirsh, J. Interactions of warfarin with drugs and food. *Ann. Intern. Med.* **1994**, *121*, 676−683. (d) Hyers, T. M. Management of venous thromboembolism. Past, present and future. *Arch. Intern. Med.* **2003**, *163*, 759−768.

(5) Pohlmann, J.; Straub, A.; Lampe, T.; Roehrig, S.; Schlemmer, K.-H.; Perzborn, E. 3-Aminophthalimide derivatives as a new class of potent inhibitors of factor Xa. Unpublished results.

(6) (a) Pinto, D. J. P.; Orwat, M. J.; Wang, S. G.; Fevig, J. M.; Quan, M. L.; Amparo, E.; Cacciola, J.; Rossi, K. A.; Alexander, R. S.; Smallwood, A. M.; Luettgen, J. M.; Liang, L.; Aungst, B. J.; Wright, M. R.; Knabb, R. M.; Wong, P. C.; Wexler, R. R.; Lam, P. Y. S. Discovery of 1-[3-(aminomethyl)phenyl]-N-[3-fluoro-2′-(methylsulfonyl)-[1,1′-biphenyl]-4-yl]-3-(trifluoromethyl)-1H-pyrazole-5-carboxamide (DPC423), a highly potent, selective, and orally bioavailable inhibitor of blood coagulation factor Xa. *J. Med. Chem.* **2001**, *44*, 566−578. (b) Lam, P. Y.; Clark, C. G.; Li, R.; Pinto, D. J.; Orwat, M. J.; Galemmo, R. A.; Fevig, J. M.; Teleha, C. A.; Alexander, R. S.; Smallwood, A. M.; Rossi, K. A.; Wright, M. R.; Bai, S. A.; He, K.; Luettgen, J. M.; Wong, P. C.; Knabb, R. M.; Wexler, R. R. Structure-based design of novel guanidine/benzamidine mimics: potent and orally bioavailable factor Xa inhibitors as novel anticoagulants. *J. Med. Chem.* **2003**, *46*, 4405−4418.

(7) Hilgers, A. R.; Smith, D. P.; Biermacher, J. J.; Day, J. S.; Jensen, J. L.; Sims, S. M.; Adams, W. J.; Friis, J. M.; Palandra, J.; Hosley, J. D.; Shobe, E. M.; Burton, P. S. Predicting Oral Absorption of Drugs: A Case Study with a Novel Class of Antimicrobial Agents. *Pharm. Res.* **2003**, *20*, 1149−1155.

(8) The correct stereochemistry of **5** was confirmed by X-ray crystallography.

(9) Weinz, C.; Buetehorn, U.; Daehler, H.-P.; Kohlsdorfer, C.; Pleiss, U.; Sandmann, K.-H.; Schwarz, T.; Steinke, W. Pharmacokinetics of BAY 59-7939 − an oral, direct Factor Xa inhibitor − in rats and dogs. *Pathophysiol. Haemost. Thromb.* **2004**, *33* (suppl. 2), PO054.

(10) Perzborn, E.; Strassburger, J.; Wilmen, A.; Lampe, T.; Pernerstorfer, J.; Pohlmann, J.; Roehrig, S.; Schlemmer, K.-H.; Straub, A. Biochemical and pharmacologic properties of BAY 59-7939, an oral, direct Factor Xa inhibitor. *Pathophysiol. Haemost. Thromb.* **2004**, *33* (suppl. 2), PO079.

(11) Gutcait, A.; Wang, K.-C.; Liu, H.-W.; Chern, J.-W. Studies on quinazolines. 6. Asymmetric synthesis of (*S*)-(+)- and (*R*)-(−)-3-[[4-(2-methoxyphenyl)piperazin-1-yl]methyl]-5-methylthio-2,3-dihydroimidazo[1,2-c]quinazolines. *Tetrahedron Asym.* **1996**, *7*, 1641−1648.

(12) Brickner, S. J.; Hutchinson, D. K.; Barbachyn, M. R.; Manninen, P. R.; Ulanowicz, D. A.; Garmon, S. A.; Grega, K. C.; Hendges, S. K.; Toops, D. S.; Ford, C. W.; Zurenko, G. E. Synthesis and Antibacterial Activity of U-100592 and U-100766, Two Oxazolidinone Antibacterial Agents for the Potential Treatment of Multidrug-Resistant Gram-Positive Bacterial Infections. *J. Med. Chem.* **1996**, *39*, 673−679.

(13) Straub, A.; Lampe, T.; Pohlmann, J.; Roehrig, S.; Perzborn, E.; Schlemmer, K.-H.; Pernerstorfer, J. Substituierte Oxazolidinone und ihre Verwendung. PCT Int. Appl. WO 01/47919. *Chem. Abstr.* **2001**, *135*, 92625.

(14) Aitken, R. A.; Bibby, M. C.; Bielefeldt, F.; Double, J. A.; Laws, A. L.; Mathieu, A. L.; Ritchie, R. B.; Wilson, D. W. J. Synthesis and Antitumour Activity of New Derivatives of Flavone-8-acetic Acid (FAA). Part 31: 2-Heteroaryl Derivatives. *Arch. Pharm. (Weinheim)* **1998**, *331*, 405−411.

(15) The X-ray crystal structure of **5** in complex with human FXa was performed by Proteros Biostructures GmbH in Planegg-Martinsried, Germany.

(16) Adler, M.; Kochanny, M. J.; Ye, B.; Rumennik, G.; Light, D. R.; Biancalana, S.; Whitlow, M. Crystal Structures of Two Potent Nonamidine Inhibitors Bound to Factor Xa. *Biochemistry* **2002**, *41*, 15514−15523.

(17) (a) Choi-Sledeski, Y. M.; Kearney, R.; Poli, G.; Pauls, H.; Gardner, C.; Gong, Y.; Becker, M.; Davis, R.; Spada, A.; Liang, G.; Chu, V.; Brown, K.; Collussi, D.; Leadley, R., Jr.; Rebello, S.; Moxey, P.; Morgan, S.; Bentley, R.; Kasiewski, C.; Maignan, S.; Guilloteau, J.-P.; Mikol, V. Discovery of an Orally Efficacious Inhibitor of Coagulation Factor Xa Which Incorporates a Neutral P1 Ligand. *J. Med. Chem.* **2003**, *46*, 681−684. (b) Maignan, S.; Guilloteau, J.-P.; Choi-Sledeski, Y. M.; Becker, M. R.; Ewing, W. R.; Pauls, H. W.; Spada, A. P.; Mikol, V. Molecular Structures of Human Factor Xa Complexed with Ketopiperazine Inhibitors: Preference for a Neutral Group in the S1 Pocket. *J. Med. Chem.* **2003**, *46*, 685−690.

(18) Tucker, T. J.; Brady, S. F.; Lumma, W. C.; Lewis, S. D.; Gardell, S. J.; Naylor-Olsen, A. M.; Yan, Y.; Sisko, J. T.; Stauffer, K. J.; Lucas, B. J.; Lynch, J. J.; Cook, J. J.; Stranieri, M. T.; Holahan, M. A.; Lyle, E. A.; Baskin, E. P.; Chen, I.-W.; Dancheck, K. B.; Krueger, J. A.; Cooper, C. M.; Vacca, J. P. Design and Synthesis of a Series of Potent and Orally Bioavailable Noncovalent Thrombin Inhibitors That Utilize Nonbasic Groups in the P1 Position. *J. Med. Chem.* **1998**, *41*, 3210−3219.

(19) Stubbs, M. T.; Reyda, S.; Dullweber, F.; Möller, M.; Klebe, G.; Dorsch, D.; Mederski, W. W. K. R.; Wurziger, H. pH-Dependent Binding Modes Observed in Trypsin Crystals: Lessons for Structure-Based Drug Design. *ChemBioChem* **2002**, *3*, 246−249.
(20) Maignan, S.; Guilloteau, J.-P.; Pouzieux, S.; Choi-Sledeski, Y. M.; Becker, M. R.; Klein, S. I.; Ewing, W. E.; Pauls, H. W.; Spada, A. P.; Mikol, V. Crystal Structures of Human Factor Xa Complexed with Potent Inhibitors. *J. Med. Chem.* **2000**, *43*, 3226−3232.
(21) (a) Berry, C. N.; Girard, D.; Lochot, S.; Lecoffre, C. Antithrombotic actions of argatroban in rat models of venous, 'mixed' and arterial thrombosis, and its effects on the tail transection bleeding time. *Br. J. Pharmacol.* **1994**, *113*, 1209−1214. (b) Sato, K.; Taniuchi, Y.; Kawasaki, T.; Hirayama, F.; Koshio, H.; Matsumoto, Y. Relationship between the antithrombotic effect of YM-75466, a novel factor Xa inhibitor, and coagulation parameters in rats. *Eur. J. Pharmacol.* **1998**, *347*, 231−236.
(22) Brandstetter, H.; Kuehne, A.; Bode, W.; Huber, R.; von der Saal, W.; Wirthensohn, K.; Engh, A. E. X-ray Structure of Active Site-inhibited Clotting Factor Xa. *J. Biol. Chem.* **1996**, *271*, 29988−29992.
(23) Reppe, W. Äthinylierung. *Liebigs Ann. Chem.* **1955**, *596*, 209.

JM050101D